Asian Journal of Chemistry; Vol. 36, No. 5 (2024), 1051-1055

ASIAN JOURNAL OF CHEMISTRY

https://doi.org/10.14233/ajchem.2024.31152

Controlled Magnetite Grafted Poly(glycidyl methacrylates) for Heavy Metal Absorption and Recovery *via* SET-LRP

N. HARIDHARAN

Department of Chemistry, Vel Tech Rangarajan Dr. Sagunthala R & D Institute of Science and Technology, Avadi, Chennai-600021, India

Corresponding author: E-mail: drnharidharan@veltech.edu.in

Received: 4 January 2024; *Accepted*: 7 March 2024; *Published online*: 30 April 2024; AJC-21608

A versatile magnetite based stringent polymer for effective metal capture was prepared by reacting iron oxide based initiator with glycidyl methacrylate monomer *via* single-electron transfer living radical polymerization (SET-LRP) technique. The versatile grafted polymer was successfully synthesized by metal catalyzed living radical polymerization using the catalyst system Cu/N,N,N′,N″,N‴-pentamethyldiethylenetriamine as the ligand. The structural confirmation of the initiator and the grafted polymer was analyzed by using instrumentation methods such as proton nuclear magnetic resonance spectroscopy, UV-visible, TGA, SEM and gel permeation chromatography for molecular weight measurements. As the polymerization time increased, both the conversion and the molecular weight were observed to increase linearly with time. Narrow dispersed lower polydispersity index (PDI) and dispensable magnetite-*g*-PGMA was utilized for the extract of toxic lead from the wastewater. Sustained binding was observed due to the presence of epoxide ring in the repeating units of the polymer and recovered by magnetic effect. The material shows good stability as evident by TGA curves and better affinity to toxic lead as observed by UV-visible and SEM techniques.

Keywords: Controlled radical polymerization, Living radical polymerization, Glycidyl methacrylate, Metal capture, Magnetite.

INTRODUCTION

A severe pollution problem especially arises due to the toxic metals ion contamination especially the lead metal in various sectors causes crucial and immediate damage to the environment [1]. More modern methodologies and treatment are involved in the specific targeting of metal ions with economic approach. Even though there are more established processes *e.g.* chemical precipitation, reverse osmosis and electrochemical treatment, adsorption is regarded as one of the most effective techniques [2].

Approaches utilizing nanoscience have demonstrated extraordinary efficacy in solving environmental problems in recent times [3]. Nanomaterial based adsorbents have demonstrated much better handling, efficiency and environmental friendliness. The adsorbents based on nanomaterials offer additional benefits because of their high surface-to-volume ratio [4]. Magnetite based nanoparticles have been extensively investigated due to its unique characteristic properties relative to magnetic interaction [5]. The properties of magnetite nanoparticles can be well tuned by adjusting the morphology and chemical compositions. Magnetite nanoparticle also possess set of features including biocompatibility, physico-chemical stability and low toxicity, so it is well suitable to act as a photo catalyst and sorbent. Magnetite in combination with polymers helps to fine-tune the properties and also for enhanced functionalization and dispersion [6-10]. The polymer provides steric stabilization and also improved the surface coating for various applications.

One of the significant polymers in the fields of material science and polymer chemistry is poly(glycidyl methacrylate) (PGMA), which finds use in the manufacturing of polymer coatings, adhesives and plastics. The pendant epoxides present in the repeating units of the polymer make it a convenient for conjugating various functional moieties. The creation of this kind of smart material, which is made up of particular polymeric components such magnetite nanoparticle surfaces and glycidyl methacrylate, provides advantages for sorption and recovery in a variety of environmental applications [11]. By using controlled radical polymerization, polymers may be synthesized conveniently and with good control over molecular weight and polydispersity index (PDI). When compared to

traditional radical polymerization, single electron transfer living radical polymerization (SET-LRP) [12,13] is one of the most effective controlled/living radical polymerization (CLRP) [14] techniques. The capability of SET-LRP to regulate and modulate molecular weight and functioning is one of its advantages. Additionally, a broad variety of functional groups in the initiator, monomer or solvent can be tolerated. The SET-LRP method is less prone to side reactions and radical termination because some of the process functions *via* outer sphere electron transfer, as opposed to the normal ATRP, which is thought to occur *via* inner sphere election transfer (where the activation of R-X by Cu(I) and subsequent generation of Cu(II) is accompanied by a halogen bridged transition state). Nguyen & Percec [15] proposed a novel technology that comprised a simple way for energizing Cu(0) wire to dramatically accelerate the SET-LRP of methyl acrylate. This approach led to high chain end functionality and superior molecular weight distribution management and a means of enhancing polymerization initiator efficiency using electronic chain end mimics.

Rehan *et al.* [16] utilized PGMA based hybrid material for the evaluation of methylene blue adsoprtion. Maximum adsorption capacity of polymer composite were found to be 76.51 and 125.95 mg/g respectively. Yeshchanko *et al.* [17] reported reported that the nanocomposite films can be effectively used as sensing elements in a low cost sensory device operating in visual lights. Xu *et al.* [18] utilized PGMA and polypropylene carboxy nitrile rubber crosslinked thermoplastic elastomer to study the effects of thermodynamic and kinetic factors on the crystallization behaviour of PP-*g*-PGMA. Jiang *et al.* [19] reported the AGET ATRP of GMA followed by ring opening reactions to facilitate self-healing nanocomposite hydrogel with the help of surface modifications of cellulose nanocrystals. The material provides outstanding auto remediation and enhanced mechanical strength for the development of CNC-based functional materials.

In present work, the metal catalyzed living polymerization of magnetite grafted poly(glycidyl methacrylate) (PGMA) with glycidyl methacrylate, at ambient temperature (30 ± 1 ºC) is reported. A magnetite initiator, Cu(0)/PMDETA catalyst system in DMSO is handled. The initiator synthesis involves the usage of 3-aminopropyltriethoxy silane and 2-bromoisobutyrl bromide [20] (Fig. 1). The magnetite-*g*-PGMA obtained through SET-LRP is utilized for environmental remedies especially capture and storage of toxic heavy metal ion from the contaminated water.

EXPERIMENTAL

Monomer glycidyl methacrylate (GMA) was purchased from Sigma-Aldrich Chemicals Pvt. Ltd. and the inhibitor was removed by passing through aluminum oxide column and then purged with argon gas. Magnetite nanoparticle Bromoisobutryl bromide, Cu(I)Br and pentamethylenediethylenetriamine purchased from Aldrich were used exactly as supplied, whereas DMSO, triethylamine and other solvents were distilled and used.

Characterization: The ^{1}H NMR spectrum was recorded on a Bruker Avance 400 spectrometer, measured in $CDCl_3$ at room temperature. UV-Visible absorbtion spectra were measured on a JASCO UV-Visible 530 spectrometer. The molecular weight measurements were obtained using a WATERS GPC equipped with three columns connected in series. Tetrahydrofuran was used as eluent and the flow rate was 1 mL/min. A refractive index detector (2410 WATERS) was used for detection and the calibration was done with narrow molecular weight polystyrene standards, whereas the data analysis was performed with standard software.

General procedure for synthesis

Synthesis of magnetite initiator: In a three-necked round bottom flask, amine terminated magnetite nanoparticles (0.2 mol), triethylamine (0.22 mol) and THF (400 mL) were inserted. While stirring, 0.22 mol of 2-bromoisobutyl bromide was gently added. The mixture was stirred for 6 h before being allowed to react. A brown precipitated triethylammonium bromide was discarded by filteration, whereas THF was removed by rotary evaporation. The final purified product was characterized by various instrumentation methods.

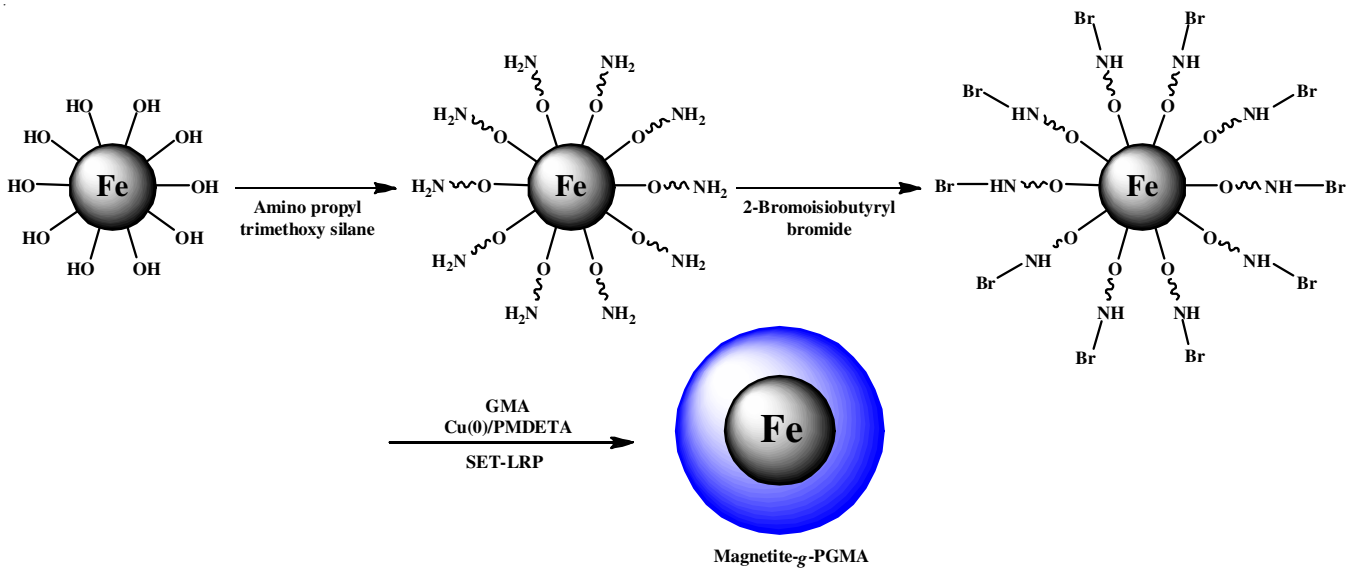

Fig. 1. Schematic illustration for the preparation of magnetite-*g*-PGMA nanocomposite

Synthesis of homopolymer *via* ATRP: In a flame dried Schlenk tube fitted with a magnetic stirring bar, the copper catalyst in DMSO was introduced. After sealing the flask with a rubber septum, it was emptied and backfilled with argon twice. A catheter was then used to introduce degassed monomer (glycidyl methacrylate, GMA). After the addition of ligand, the solution was agitated until the copper complex formed. Following the formation of the complex, the magnetite initiator was added and the mixture was agitated at room temperature. The polymerization was terminated after the set time period by diluting with THF solvent. Methanol was used to precipitate the polymer, which was then dried under vacuum. Filtration using a neutral alumina column removed the copper complex from polymer. The polymer solution was utilized to calculate the molecular weight and polydispersity index (PDI) and the polymer was characterized using spectroscopic techniques.

RESULTS AND DISCUSSION

In an attempt to investigate the efficiency of the magnetite polymer and the recovery of toxic heavy metal, metal catalyzed living polymerization of glycidyl methacrylate (GMA) were performed at ambient temperature. The production of homo polymer is further verified by the ^{1}H NMR spectrum (Fig. 2), which reveals six strong peaks at 0.89, 1.83, 4.2, 3.2, 2.81 and 3.72 ppm, corresponding to methyl and methylene protons. The signal at 2.81 ppm, which corresponds to the epoxide methylene group, demonstrates the successful polymer synthesis on the initiator site.

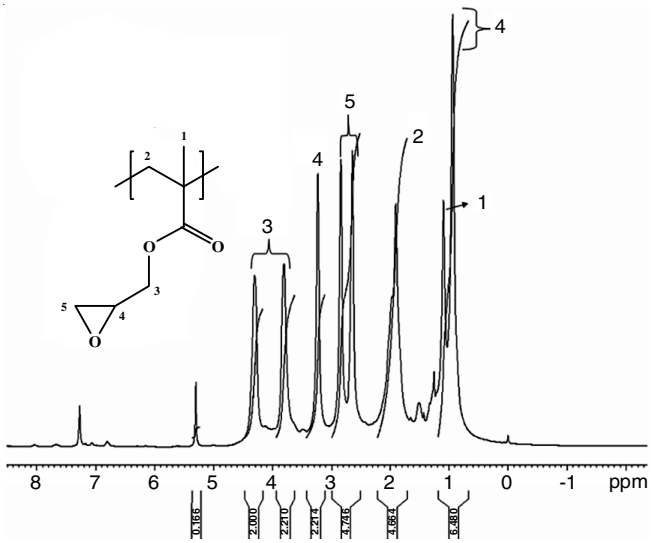

Fig. 2. ^{1}H NMR spectrum of the magnetite-*g*-PGMA homopolymer

Tables 1 and 2 show the results of the polymerization of GMA in bulk and solution (anisole 50% v/v). The results showed that as the polymerization time rises, so does the percentage of monomer conversion and the molecular weight. The PDI obtained in solution is nearly identical to that obtained in bulk. However, the solvent produced a near match between Mn theory and Mn GPC values. Polymerization of GMA in bulk results in 90% conversion in 50 min compared to 40% conversion in solution polymerization, indicating that the rate of polymerization of GMA in bulk is significantly quicker and more controllable. It also appears to be more regulated as observed by the lower PDI levels. This might be owing to the catalyst system in GMA being more soluble in solution than in bulk. In terms of PDI values for the produced polymers, GMA polymerization is highly regulated both in bulk and in solvent. However, solution polymerization produced a better match between theoretical and expected GPC values. The single electron transfer live radical polymerization technique with reduced PDI values was used to effectively manufacture well-controlled PGMA.

TABLE-1
LARGE SCALE GMA POLYMERIZATION AT AMBIENT TEMPERATURE TARGET DEGREE OF POLYMERIZATION = 400

Cu(0):L	Time (min)	Conv. (%)	M_n (Expected)[a]	M_nGPC[b]	PDI
1:1	10	32.0	18176	17860	1.3
1:1	20	48.0	27264	24800	1.34
1:1	30	67.0	38056	31680	1.36
1:1	40	84.0	47712	40070	1.38
1:1	50	95.0	53960	–	High PDI

[a]Molecular weight of the monomer × conversion yield × $[M]_o/[I]_o$
[b]Polystyrene calibration standard.

TABLE-2
POLYMERIZATION OF GMA PERFORMED IN SOLUTION MEDIUM AT AMBIENT TEMPERATURE IN DMSO (50%V/V). TARGET DEGREE OF POLYMERIZATION = 400

Cu(0):L	Time (h)	Conv. (%)	M_n (Expected)[a]	M_nGPC[b]	PDI
1:1	8	40.0	22720	21800	1.26
1:1	16	49.7	28300	26000	1.28
1:1	24	58.4	33200	30500	1.33
1:1	32	65.0	37000	33700	1.35
1:1	45	74.6	42400	37000	1.38

[a]Molecular weight of monomer × conversion yield × $[M]_o/[I]_o$
[b]Polystyrene calibration standard.

Thermal studies: Thermogravimetric studies were done for the magnetite initiator and the polymer composite to analyses the degradation and strength of the synthesized material as shown in Fig. 3. The magnetite nanoparticle, bromine end functionalized magnetite initiator and the polymer nanocomposite were shown different degradation with respect to the temperature. The curve initially shows a 25% reduction in the overall weight, which might be explained by the loss of molecules of amino propyl, bromide and adsorbed water from the surface of the nanoparticles. The PGMA-grafted magnetic nanoparticles' curve shows one minor area and two major zones of weight reduction. One can attribute the loss of remaining monomer and adsorbed water to roughly 160 ºC. The breakdown of the initiator moiety on the magnetite surface is responsible for the larger weight loss area about 260 ºC. A significant breakdown of the polymer chains in the composite material causes a 70% total weight reduction, with the main region of this breakdown occurring at 355 ºC.

Molecular modeling: Three dimensional molecular interactions of metal ion with magnetite-*g*-polymer composite are depicted in Fig. 4, mainly due to presence of electrostatic forces and the formation of coordinating bonds linking the metal and

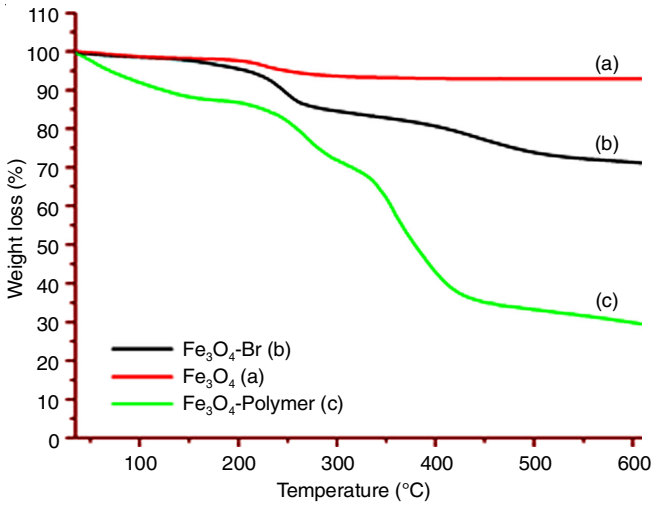

Fig. 3. Thermal measurements for the magnetite initiator and its related polymer nanocomposite

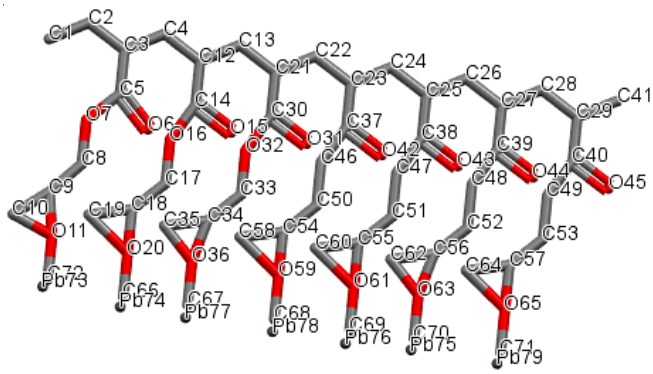

Fig. 4. Molecular modeling for the arrangement of polymer and its interaction with lead ion

the composite. The bonding between metal ion and the polymer composite may also occur due to the weak interactions such as trapping metal ions in the bulk of the polymer phase. The less hindered β-carbon atom of epoxide is vulnerable to assaults by metal ions, which can result in epoxide ring opening and the production of a metal-ligand intermediate.

Metal binding studies: The UV-visible characterization is useful to analyze the binding affinity of the polymer composite with the metal ion and easy recovery by magnetic effect. Fig. 5 illustrates the absorption spectra pattern for the interaction of the polymer composite with lead ion. The spectra shows two peaks results from the interaction, the peak at 380 nm was in lower intensity, however the peak at 300 nm was very broad and in higher intensity. The binding studies were examined using different mole equivalents of toxic lead ion ranging from 0.2 to 1.0 equiv. with respect to 10^{-5} mol L^{-1}. The metal ion interaction with PGMA is more significant and the absorption is blue shifted in the spectra implied that the polymer's epoxide ring had a stronger potential to interact with lead compared to the alkyl group. The metal-polymer interaction increases with decreases in the absorption intensity of the spectra as shown in Fig. 5.

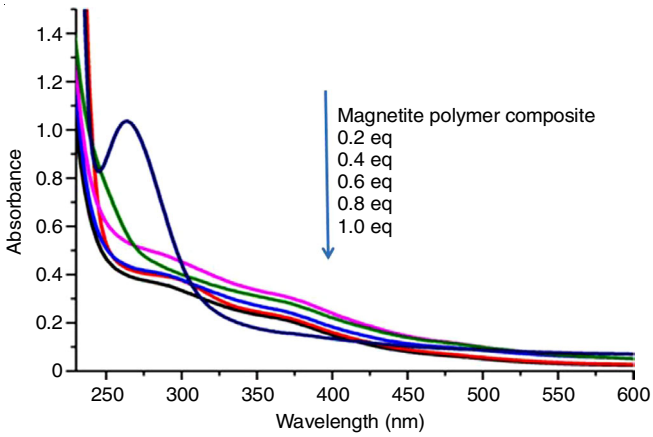

Fig. 5. UV-vis studies for the interactions of magnetite-*g*-poly(GMA) in tetrahydrofuran at a concentration of 10^{-5} mol L^{-1} with lead acetate

Morphological studies: The morphological features of the polymer nanocomposite were analyzed by SEM images as shown in Fig. 6. The magnetic PGMA microspheres made by SET-LRP have an indefinite and variable size and shape with more spheres and flakes like structure. Further, the nanocom-

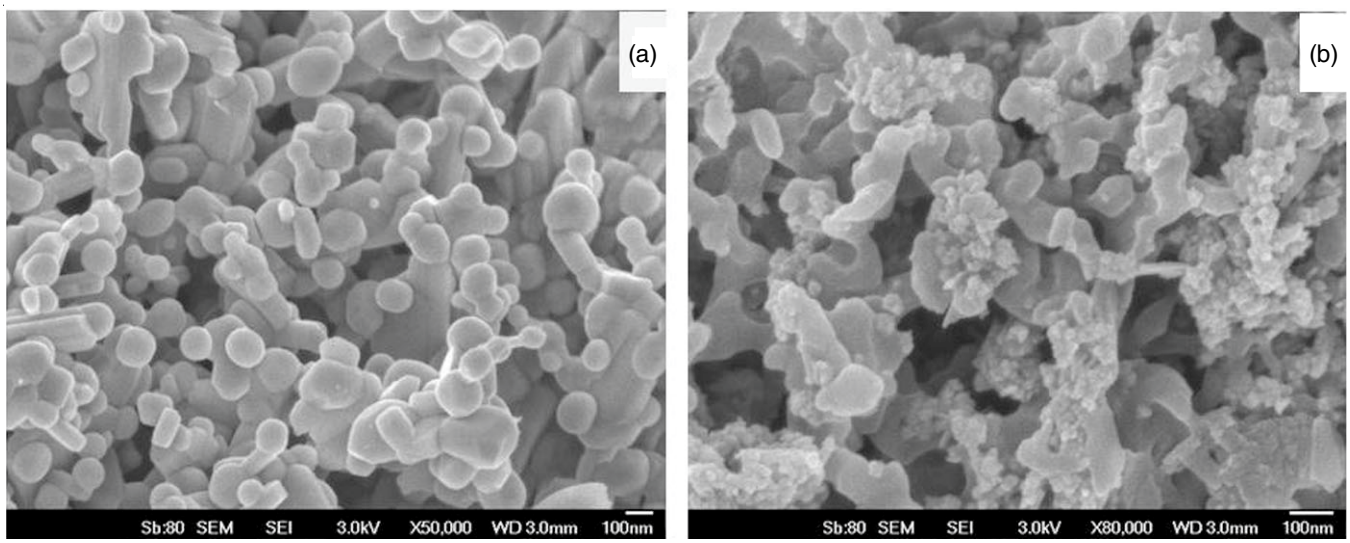

Fig. 6. SEM morphological images of polymer nanocomposite before (a) and after (b) binding metal ion

posite material synthesized will be magnetic in nature and the polymer particles magnetism content is usually unequal [21]. The images clearly illustrated that binding shows more irregular shapes due to the interaction of lead ion with the surface of nanocomposite (b) in comparison to the morphology of nanocomposite, which shows regular sphere array for the PGMA nanocomposite (a).

Conclusion

Controlled synthesis of magnetite-*g*-PGMA with specified molecular weight and narrow polydispersity with free epoxide rings was accomplished at ambient temperature using SET-LRP and a magnetite-based initiator. Kinetic and molecular weight investigations indicated that the initiator is effective as an ambient temperature SET-LRP initiator. The adaptability of the initiator, thermal stability, molecular modeling, shape and metal ion binding property were all thoroughly investigated. The material shows stability over 600 ºC with a overall weight loss of 70%. Well-controlled and dispersable magnetite-*g*-PGMA was utilized for the removal of toxic lead ions from the pollutant water. The polymer nanocomposite interacts with lead significantly and the absorption is blue shifted in the spectra. The sustained binding was observed due to the presence of epoxide ring in the repeating units of polymer and recovered by magnetic effect.

ACKNOWLEDGEMENTS

The author thank Vel Tech Rangarajan Dr. Sagunthala R&D Institute of Science and Technology for the financial support from Seed Grant No. VTU SEED (FY-22-23)-06.

CONFLICT OF INTEREST

The authors declare that there is no conflict of interests regarding the publication of this article.

REFERENCES

1. J. Briffa, E. Sinagra and R. Blundell, *Heliyon*, **6**, e04691 (2020); https://doi.org/10.1016/j.heliyon.2020.e04691
2. N.E. Hira, S.S.M. Lock, N.F. Shoparwe, I.S.M. Lock, L.G. Lim, C.L. Yiin, Y.H. Chan and M. Hassam, *Sustainability*, **15**, 1510 (2023); https://doi.org/10.3390/su15021510
3. L. Pokrajac, A. Abbas, W. Chrzanowski, G.M. Dias, B.J. Eggleton, S. Maguire, E. Maine, T. Malloy, J. Nathwani, L. Nazar, A. Sips, J. Sone, A. van den Berg, P.S. Weiss and S. Mitra, *ACS Nano*, **15**, 18608 (2021); https://doi.org/10.1021/acsnano.1c10919
4. H. Sadegh, G.A.M. Ali, V.K. Gupta, A.S.H. Makhlouf, R. Shahryari-Ghoshekandi, M.N. Nadagouda, M. Sillanpää and E. Megiel, *J. Nanostruct. Chem.*, **7**, 1 (2017); https://doi.org/10.1007/s40097-017-0219-4
5. A.G. Niculescu, C. Chircov and A.M. Grumezescu, *Methods*, **199**, 16 (2022); https://doi.org/10.1016/j.ymeth.2021.04.018
6. Q. Lu, K. Choi, J.D. Nam and H.J. Choi, *Polymers*, **13**, 512 (2021); https://doi.org/10.3390/polym13040512
7. S.H. Kwon, J.S. An, S.Y. Choi, K.H. Chung and H.J. Choi, *Macromol. Res.*, **27**, 448 (2019); https://doi.org/10.1007/s13233-019-7065-9
8. M. Ul-Islam, M.W. Ullah, S. Khan, S. Manan, W.A. Khattak, W. Ahmad, N. Shah and J.K. Park, *Environ. Sci. Pollut. Res. Int.*, **24**, 12713 (2017); https://doi.org/10.1007/s11356-017-8765-3
9. D.E. Park, H.S. Chae, H.J. Choi and A. Maity, *J. Mater. Chem. C Mater. Opt. Electron. Devices*, **3**, 3150 (2015); https://doi.org/10.1039/C5TC00007F
10. Y.Z. Dong and H.J. Choi, *Macromol. Res.*, **26**, 667 (2018); https://doi.org/10.1007/s13233-018-6097-x
11. L. Mohammed, H.G. Gomaa, D. Ragab and J. Zhu, *Particuology*, **30**, 1 (2017); https://doi.org/10.1016/j.partic.2016.06.001
12. X. Jiang, J.B. Mietner, C. Harder, R. Komban, S. Chen, C. Strelow, U. Sazama, M. Fröba, C. Gimmler, P. Müller-Buschbaum, S.V. Roth and J.R.G. Navarro, *ACS Appl. Mater. Interfaces*, **15**, 5687 (2023); https://doi.org/10.1021/acsami.2c20775
13. G. Lligadas, S. Grama and V. Percec, *Biomacromolecules*, **18**, 2981 (2017); https://doi.org/10.1021/acs.biomac.7b01131
14. W.A. Braunecker and K. Matyjaszewski, *Prog. Polym. Sci.*, **32**, 93 (2007); https://doi.org/10.1016/j.progpolymsci.2006.11.002
15. N.H. Nguyen and V. Percec, *J. Polym. Sci. A Polym. Chem.*, **48**, 5109 (2010); https://doi.org/10.1002/pola.24309
16. K.M. Rehan, K.A. Basha and S.M. Safiullah, *J. Inorg. Organomet. Polym. Mater.*, **33**, 2172 (2023); https://doi.org/10.1007/s10904-023-02671-3
17. O.A. Yeshchenko, S.Z. Malynych, S.O. Polomarev, Y. Galabura, G. Chumanov and I. Luzinov, *RSC Adv.*, **9**, 8498 (2019); https://doi.org/10.1039/C9RA00498J
18. X. Xu, J. Qiao, J. Yin, Y. Gao, X. Zhang, Y. Ding, Y. Liu, Z. Xin, J. Gao, F. Huang and Z. Song, *J. Polym. Sci. B, Polym. Phys.*, **42**, 1042 (2004); https://doi.org/10.1002/polb.10694
19. C. Jiang, W. Fan, N. Zhang, G. Zhao, W. Wang, L. Bai, H. Chen and H. Yang. *Hydrogels*, **28**, 9785 (2021); https://doi.org/10.1007/s10570-021-04170-5
20. R.A. Bini, R.F.C. Marques, F.J. Santos, J.A. Chaker and M.M. Jafelicci Jr., *J. Magn. Magn. Mater.*, **324**, 534 (2012); https://doi.org/10.1016/j.jmmm.2011.08.035
21. H. Cong, B. Yu, L. Gao, B. Yang, F. Gao, H. Zhang and Y. Liu, *RSC Adv.*, **8**, 2593 (2018); https://doi.org/10.1039/C7RA13158E